A Vision-based Autonomous Lane Following System for a Mobile Robot

Xia Huang

Department of Electrical and Computer Engineering
Purdue University Calumet
Hammond, IN, USA

Nasser Houshangi

Department of Electrical and Computer Engineering
Purdue University Calumet
Hammond, IN, USA

Abstract—In this paper, a vision-based autonomous lane following system for a mobile robot is presented. To achieve the autonomous lane following, the lane images are obtained in real time using a camera fixed mounted on the robot. Lane position is presented based on Lane Boundary Pixel Extractor (LBPE) and Hough Transform in the image coordinate frame, and transformed to the mobile robot coordinate frame using photogrammetric techniques. The visibility of the lane information is checked by the lane width constraints and its parallel property. Path planning of the mobile robot is performed based on mobile robot's position and orientation with respect to the lanes obtained from the vision information. Experimental results demonstrated the feasibility of the approach.

Keywords—**Mobile Robot, Vision, Camera Calibration, Lane Following.**

I. INTRODUCTION

Vision is an essential information source for the autonomous ground vehicle (AGV) navigation applications. The primary task of vision is to provide a description of the world rich enough to facilitate such behavior as road-following, obstacle avoidance, landmark recognition, and cross-country navigation [1]. There has been previous research on the vision-based navigation solutions. A visual servoing approach is presented in [2] to solve the path following control law directly in the image plane, thus without decomposing the problem into the lane detection and lane following subproblems. The vision module of Vision Task Sequencer (VITS) [1] generating a description of the road is transformed by the reasoning module into world coordinates to calculate the trajectory of the robot. The current motivation is to improve AGVs navigation techniques by expanding their autonomy, capabilities and their usefulness [3].

Lane following based on the relative position between the lane boundaries and a vehicle has been a well-known method for navigation because of its simple concept [5, 7]. Another advantage of this method is that the vision information can later be integrated with inertial and odometry data to improve the vehicle's performance [12, 13].

For a given image, the challenge is how to obtain the accurate lane related parameters. A typical method is to extract the pixels expected to be on the lane boundaries by a LBPE [4] and then estimate the lane-related parameters using Hough Transform [5]. However, this method is greatly influenced by

the LBPE. The approach in [6] increases the number of lane-related parameters and introduces departure ratios to determine the instant of lane departure and a Linear Regression (LR) to minimize wrong decisions due to noise effects. Furthermore, to prevent the false alarms and detection misses, the LR of lane-related parameters are obtained form a few successive images instead of a single frame.

In this research, lane information is detected based on the algorithm presented in [6] and transformed to the mobile robot coordinate frame through an optimal camera calibration process. Four criteria are defined based on the lane width constraints and its parallel property to check the reliability of the vision information. Based on the mobile robot's position with respect to the lanes, the planner generates the desired trajectory for the robot to navigate between the two lanes autonomously. The proposed approach is experimentally implemented using a Pioneer 2 mobile robot with a CMOS camera.

Sections II and III describes the lane position acquisition using a single camera and the estimation of the mobile robot's position and orientation in different cases. Section IV provides the integrated robot lane following process. Experimental results and conclusions are discussed in sections V and VI, respectively.

II. LANE POSITION REPRESENTATION USING A SINGLE CAMERA

Several steps are taken to detect and represent the lane position using vision information. First, the coordinate frames for the mobile robot and the camera are assigned. The camera is calibrated with respect to the mobile robot coordinate frame. The captured image from the camera is processed in the camera coordinate frame and transformed to the mobile robot coordinate frame to determine the lane position. Each step is explained as follows.

A. Coordinate frame assignment

A single camera is fixed on a stand which is attached to the front of a mobile robot as shown in Fig. 1. The mobile robot is modeled as a rigid body with two differential driving and one caster wheel. The mobile robot coordinate

frame is defined by $[X_m\ Y_m\ Z_m]$ where the origin O_m is located at the robot's kinematics center on the ground plane as shown in Fig. 1. $[X_c\ Y_c\ Z_c]$ defines the camera coordinate frame, where O_c is at the center of the image plane and the Z_c axis has the same direction as the optical axis of the camera. The camera coordinate frame is parallel to the mobile robot coordinate frame if it is rotated clockwise around the X_c axis by angle θ as shown in Fig. 1.
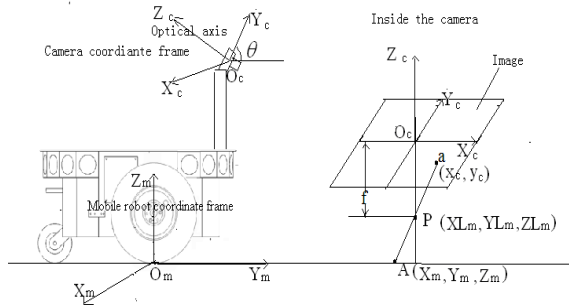

Fig. 1.   Coordinate frames for the mobile robot and the camera

B.   Camera calibration

The camera is modeled as a pin-hole camera. The perspective center P of the camera, the point A on the ground, and A's projection on the image a are connected by an image ray as shown in Fig. 1. A single image can be thought of as a bundle of such rays converging at the perspective center with an unknown position and orientation in space which can be identified by the camera calibration process [8]. Points "A", and "P" are represented by $(X_m\ Y_m\ Z_m)$, and $(XL_m\ YL_m\ ZL_m)$ in the mobile robot coordinate frame, respectively. Point "a" is specified by (x_c, y_c) in the camera coordinate frame. The collinearity equation which establishes the relationship between the two coordinate frames is:

$$\overline{Pa} = \lambda \overline{AP} \qquad (1)$$

where λ is the constant scale factor. Equation (1) can be rewritten as:

$$\begin{bmatrix} x_c \\ y_c \\ -f \end{bmatrix} = \lambda Rot(x,\theta) \begin{bmatrix} X_m - XL_m \\ Y_m - YL_m \\ Z_m - ZL_m \end{bmatrix} \qquad (2)$$

Eliminating the scalar λ by dividing the first two rows by the third row in equation (2) results in:

$$F = \begin{bmatrix} F_x(x_c,\beta) \\ F_y(y_c,\beta) \end{bmatrix} = \begin{bmatrix} 0 \\ 0 \end{bmatrix} \qquad (3)$$

where

$$F_x(x_c,\beta) = x_c + f \frac{X_m - XL_m}{-\sin(\theta)*(Y_m - YL_m) + \cos(\theta)*(Z_m - ZL_m)}$$
$$F_y(y_c,\beta) = y_c + f \frac{\cos(\theta)*(Y_m - YL_m) + \sin(\theta)*(Z_m - ZL_m)}{-\sin(\theta)*(Y_m - YL_m) + \cos(\theta)*(Z_m - ZL_m)} \qquad (4)$$
$$\beta = [\theta, XL_m, YL_m, ZL_m, f]^T$$

It is noticed that at least five independent equations are needed to obtain the unique solution for the five unknowns in β and each point in the image can generate two equations as in (4). However, a more optimal result is found by using non-linear least square techniques with redundant observations.

The value of β is refined iteratively by successive approximation [14] as:

$$\beta^{k+1} = \beta^k + \Delta\beta \qquad (5)$$

Where k is the iteration number and $\Delta\beta$ is known as the shift vector. At each iteration, the model in (4) is linearized by keeping the first-order terms of the Taylor series expansion about β^k as:

$$F(x_{c_i}, y_{c_i}, \beta) = F_{5\times1}^k(x_{c_i}, y_{c_i}, \beta) + B_{2n\times5}\Delta\beta_{5\times1} \qquad (6)$$

where B is the matrix of the partial derivatives with respect to each unknown; n is the number of the observed points and $i = 1,...,n$. The residual is defined as the difference between the values of the dependent variable and the predicted values from the estimated model and given by:

$$r_i = F_i - (B\Delta\beta + F^k(x_{c_i}, y_{c_i}, \beta)) \qquad (7)$$
$$= -B\Delta\beta - F^k(x_{c_i}, y_{c_i}, \beta)$$

The least squares method defines the optimal solution to minimize when the sum of the squared residual $\sum_{i=1}^{2n} r_i^2$, which is   realized by setting its gradient to zero [14] and this leads to

$$\Delta\beta = (B^T B)^{-1} B^T (-F^k(x_{c_i}, y_{c_i}, \beta)) \qquad (8)$$

The algorithm terminates until $\Delta\beta$ approaches zero.

C.   Lane position representation

The inverse collinearity equations are derived from (2) as :

$$X_m = \frac{x_c}{y_c \sin\theta - f\cos\theta}(Z_m - ZL_m) + XL_m$$
$$Y_m = \frac{y_c \cos\theta + f\sin\theta}{y_c \sin\theta - f\cos\theta}(Z_m - ZL_m) + YL_m \qquad (9)$$

The values of $(XL_m, YL_m, ZL_m, \theta, f)$ are obtained from calibration process explained earlier. Therefore, for any point in the image with the pixel coordinates (x_c, y_c), its corresponding coordinates $[X_m, Y_m, Z_m]$ in the mobile robot coordinate frame can be obtained using equation (9) and Z_m is zero since the lanes are assumed on a flat surface.

At each time interval a 24 bit RGB format 360×240 pixel image of the lane is captured by the camera. The captured image is converted to grayscale image using NTSC television standard [9]. The lane parameters θ_l, θ_r, ρ_l and ρ_r shown in Fig.2 are obtained by LBPE and Hough transform [6]. θ_l and θ_r are the angles of the vectors from the origin to the closest points on the two lanes; ρ_l and ρ_r are the magnitudes of these two vectors. Points 1,2,3 and 4 are chosen to represent the two lanes and transformed to the mobile robot coordinate frame to determine the lane position.
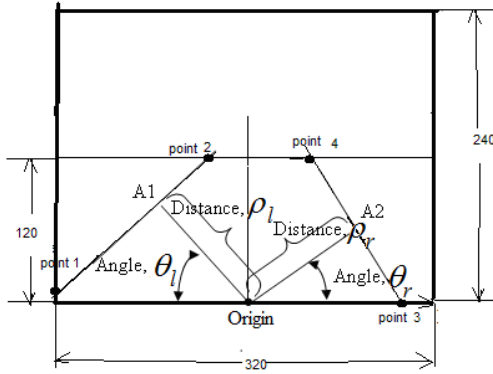
Fig. 2.   A processed RGB image

III.   MOBILE ROBOT POSITION AND ORIENTATION DETERMINATION

The objective is to navigate the mobile robot in the middle and parallel with the two lanes. The position x, and orientation φ of the mobile robot are used to indicate the displacement and angle between the mobile robot and the middle of the lanes, respectively, as shown in Fig. 3. The distances and orientation of mobile robot with respect to the left and right lane are described by x_l, x_r and φ_l, φ_r, respectively.

The four points 1,2,3 and 4 in the camera coordinate frame (see Fig. 2) are transformed to the mobile robot coordinate frame as points 1',2',3',4' (see Fig. 3) using the inverse collinearity equations described in the previous section.
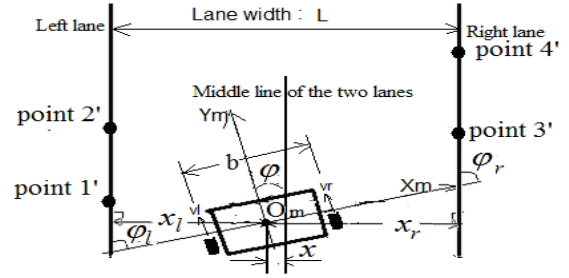
Fig. 3 Mobile robot's position and orientation with respect to the lanes

Suppose the coordinate values in the mobile robot coordinate frame for the four points shown in Fig. 3 are (X_{p1}, Y_{p1}), (X_{p2}, Y_{p2}), (X_{p3}, Y_{p3}) and (X_{p4}, Y_{p4}), respectively. Then, the mobile robot position and orientation $\hat{x}_l, \hat{x}_r$ and $\hat{\varphi}_l, \hat{\varphi}_r$ are estimated as:

$$\hat{\varphi}_l = \arctan(\frac{Y_{p2} - Y_{p1}}{X_{p2} - X_{p1}}), \ \hat{\varphi}_r = \arctan(\frac{Y_{p4} - Y_{p3}}{X_{p4} - X_{p3}})$$

$$\hat{x}_l = \frac{|Y_{p1} X_{p2} - Y_{p2} X_{p1}|}{\sqrt{(Y_{p2} - Y_{p1})^2 + (X_{p2} - X_{p1})^2}}$$

$$\hat{x}_r = \frac{|Y_{p3} X_{p4} - Y_{p4} X_{p3}|}{\sqrt{(Y_{p4} - Y_{p3})^2 + (X_{p4} - X_{p3})^2}}$$

(10)

For simplicity, it is assumed that the two lanes are parallel to each other all the time with the known lane width L. Therefore, $\hat{\varphi}_l = \hat{\varphi}_r$ and $\hat{x}_l - \frac{1}{2} = \frac{1}{2} - \hat{x}_r$. It is also assumed that the mobile robot always starts within the lanes.

Unfortunately, at any given time both left and right lanes' information may not be available due to the limitation of the scope of the visual field or the disturbances such as the light intensity and the road color. In order to determine the reliability of the lane information in different cases, four criteria are used during mobile robot navigation as follows:

a) $|\hat{\varphi}_l - \hat{\varphi}_r| < \varphi_{th}$

b) $|\hat{x}_l + \hat{x}_r - L| < x_{th}$

c) $\varphi_{th1} < |\hat{\varphi}_l| < \varphi_{th2} \quad x_{th1} < |\hat{x}_l| < x_{th2}$

d) $\varphi_{th1} < |\hat{\varphi}_r| < \varphi_{th2} \quad x_{th1} < |\hat{x}_r| < x_{th2}$

The theresholds $\varphi_{th}, x_{th}, \varphi_{th1}, \varphi_{th2}$ and x_{th1}, x_{th2} are the experimentally determined. Both lanes' information are useful if both a) and b) are true. In this case, the position and orientation of mobile robot is estimated as $\hat{\varphi} = (\hat{\varphi}_l + \hat{\varphi}_r)/2$ and $\hat{x} = (\hat{x}_l - \hat{x}_r)/2$. One or both of the lanes' information may be erroneous if either a) or b) does not hold. In this case, both c) and d) need to be checked. If only c) is true then the data from left lane is used: $\hat{\varphi} = \hat{\varphi}_l$ and $\hat{x} = \hat{x}_l - \frac{1}{2}$. If only d) is true then the data from right lane is

used: $\hat{\varphi}=\hat{\varphi}_r$ and $\hat{x}=\frac{L}{2}-\hat{x}_r$. The vision information is not useful for navigation if both c) and d) are true, or neither of them is true.

IV. MOBILE ROBOT PATH PLANNING AND NAVIGATION

As explained earlier, at each step the captured image by the camera is processed to obtain the values of $\theta_l, \theta_r, \rho_l$ and ρ_r which are used to represent the two lanes in the camera coordinate frame. This information is transformed to mobile coordinate frame and robot position and orientation with respect to the lanes are determined. Based on current and desired robot position and orientation, the planner generates the desired robot wheel velocities for the controller. The integrated robot navigation process is shown in Fig. 4.
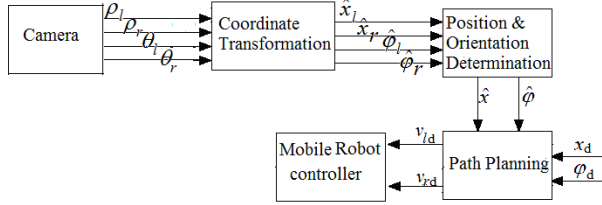

Fig. 4 Integrated robot navigation process

The mobile robot position and orientation are estimated with respect to the lanes by:

$$\begin{bmatrix} x(k+1) \\ \varphi(k+1) \end{bmatrix} = \begin{bmatrix} x(k) \\ \varphi(k) \end{bmatrix} + \begin{bmatrix} v_x(k) \\ \dot{\varphi}(k) \end{bmatrix} T_s$$

$$v_x = \frac{v_l+v_r}{2}\sin\varphi, \quad \dot{\varphi}=\frac{v_r-v_l}{b}$$

(11)

In (11), k is a positive integer and T_s is the sample period; v is the mobile robot's velocity along the X_m; $\dot{\varphi}$ is the angular velocity; v_l and v_r are the robot's left and right wheels' velocities, respectively, and b is the distance between the two wheels as shown in Fig. 3. A PID controller is used to track the desired position and orientation [10].

V. EXPERIMENTAL RESULTS

The objective of the experiment conducted is to demonstrate the feasibility of lane detection for autonomous lane navigation. The mobile robot platform used is Pioneer 2DXe which is a general purpose mobile robot from MobileRobots Inc. and the vision sensor is a V-X0097-SE Color CMOS camera as shown in Figure 5.

Fig. 5 Mobile robot with a mounted camera

The camera is fixed on a stand with a tilt angle and the stand is attached to the front of the mobile robot. The communication between the computer and the mobile robot is wireless. The image processing software is written in C++. The robot control is performed using Advanced Robot Interface for Applications (ARIA) C++ library [11].

The lane detection algorithm used in this research has a robust performance in the nighttime, raining weather, and other various conditions as shown in [6]. Due to this fact, although, the experimental results in this paper are for indoor environment, the approach can be expanded to the outdoor environment as well.

A. Camera calibration and coordinate transformation.

To calibrate the camera, the robot is placed in the middle and parallel to the lanes and an image shown in Fig. 6 is captured.

Fig. 6   An image captured by the camera

Eight points are chosen as shown in Fig. 6 and their coordinates in the camera and mobile coordinate frame are measured. The calibration parameters θ, XL_m, YL_m, ZL_m and f are obtained from procedure described earlier in section II. The angle θ shown in Fig. 1 is calculated to be 35.64^o versus the value measured by protractor as 35°.

Using the calibration parameters, the eight points' pixel values are transformed to the mobile robot coordinate frame by the inverse collinearity equations (9) to verify the calibration results. The measured lane position versus position obtained from calibrated camera is shown in Fig. 7.
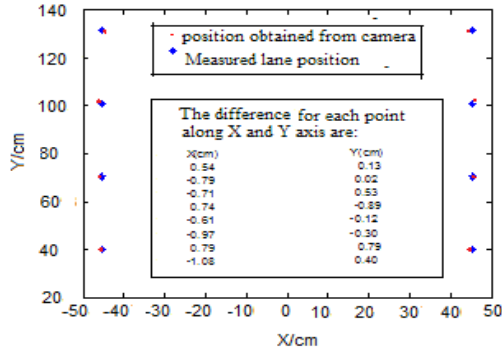

Fig. 7 Camera calibrated vs. actual position

As shown in Fig. 7, the largest difference between the actual position and position obtained from camera is $1.08cm$ which acceptable for this application.

B.   Mobile robot navigation

The robot is tested with different initial positions, and orientations for straight and curved lanes. The preliminary experiments involved controlling the robot based on a single captured image. Three cases are considered and results are shown in Figures. 8, 9, and 10. For each case the image obtained from the camera is shown in the left side while the plotting of the lane position in the mobile robot coordinate frame is shown in the right side.

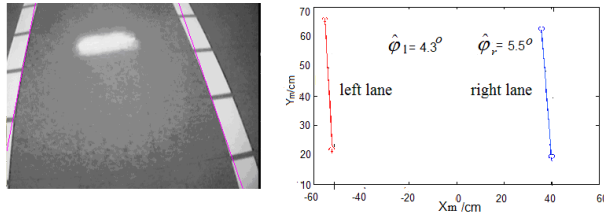Case1: The robot is in the middle with 7° orientation to the right.

Fig. 8 Lanes in the camera and the mobile robot coordinate frame for case 1

For this case, both left and right lane information are used from the captured image. As shown in Fig. 8, $\hat{\varphi}_l = 4.3^o$ and $\hat{\varphi}_r = 5.5^o$ from vision. Based on this information, the robot is commanded to become parallel with the lanes. After execution, it is observed that $\varphi = 1.3^o$.

Case2: The mobile robot is in the middle with 15° orientation to the right.
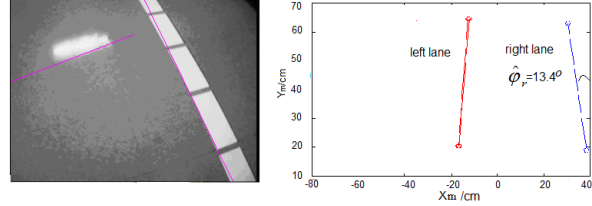

Fig. 9 Lanes in the image and the mobile robot coordinate frame for case 2.

For this case, since the left lane is not visible, the edge of the white block is detected, but this erroneous lane will be eliminated as described in section III and only the right lane information from the captured image is used. As shown in Fig. 9, $\hat{\varphi}_r = 13.4^o$ from vision. Based on this information, the robot is commanded to become parallel with the lanes. After execution, it is observed that $\varphi = 4^o$.

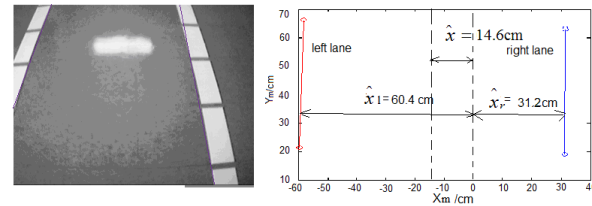Case 3: The mobile robot is placed parallel with the lanes with $12.75cm$ displacement to the right lane.

Fig. 10 Lanes in the image and the mobile robot coordinate frame for case 3

For this case both left and right lane information is useful from the captured image. As shown in Fig. 10, mobile robot's position along X_m is $\hat{x} = 14.6cm$. Based on this information, the robot is commanded to become in the middle of the lanes. After execution, it is observed that $x = 1.65cm$.

For the next set of experiments, the algorithm is implemented while continuously capturing and analyzing images. Fig. 11 shows the results under different lane configurations and initial positions and orientations.
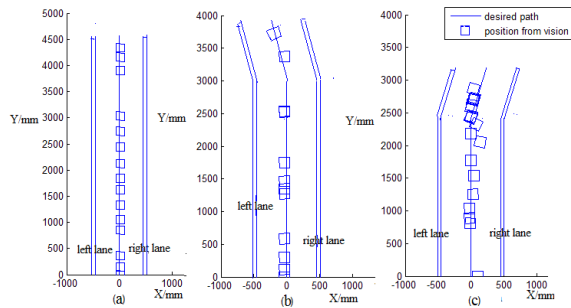
Fig. 11 (a) Straight lane; (b) Curve to the left; (c) Curve to the right

As shown in Fig. 11(a), the initial position and orientation of the mobile robot are: $x = 0, \varphi = 0$ and the lanes are straight. Figure 11(b) has the same initial condition for the mobile robot with the lanes curving to the left. In Fig. 11(c) initially $x \neq 0, \varphi = 0$ and the lane is curving to the right. The solid lines in the middle of the lanes are the desired paths and the squares represent the mobile robot's positions and orientations. It is shown that in each execution, based on the vision information the path planning algorithm tries to drive the mobile robot in the middle and parallel with the lanes.

VI. CONCLUSION

This paper presents an integrated vision-based lane following system. A robust lane detection algorithm applicable to indoor and outdoor [6] environment is used. In this paper, it is shown that the lane detection information can be used to successfully navigate the mobile robot. Mobile robot's performance depends on the visibility of the lane. In the future work, the higher rate odometry data will be integrated with vision to improve the robustness of the system.

REFERENCES

[1] Truk, M.A., Morgenthaler, D.G, Gremban, K.D., Marra, M, " VITS – A vision system for autonomous land vehicle navigation," IEEE Trans. Pattern Anal. Mach. Intell. 10(3), 342-361 (1988).

[2] Y. Ma, J. Kosecka, and S.S Sastry, "Vision guided navigation for a nonholonomic mobile robot," IEEE Transactions on Robotics and Automation, 15(3) : 521-536, June 1999.

[3] Francisco, B.F., Alberto, O., Gabriel O, "Visual Navigation for Mobile Robots: A Survey," J Intell Robot Syst. 263-296 (2008)

[4] Lee J. W., Lee, U.K., Yi, "A new approach for lane departure identification," Proc. IEEE Intelligent Vehicles, 100-105 (2003)

[5] Pomerleau, D.A., Jochem, T, "Rapidly adapting machine vision for automated vehicle steering," IEEE Expert Intelligent Systems and Their Application, 19-27 (1996)

[6] Lee, J. W., Yi, U. K, "A lane departure identification based on LBPE, Hough transform, and linear regression," Computer Vision and Automation Magazine, June 2006, pp. 359-383.

[7] Brattoli, M., Tasca, R., Tomasini, A., Chioffi, E., Gerna, D., Pasotti, M, "A vision-based alert system" Proc. IEEE Intelligent Vehicles, 195-200 (1996)

[8] Edward M.Mikhail, James S. Bethel and J. Chris McGlone, *Introduction to Modern Photogrammetry.* John Wiley & Sons, Inc, 2001.

[9] Gernot Hoffmann, "Luminance models for grayscale conversions," [Online].Available: http://www.fho-emden.ed/~hoffmann/gray10012001.pdf.

[10] Pioneer 2/ PeopleBot Operations Manual [Online]. Available: http://www-ee.ccny.cuny.edu/www/web/jxiao/P2-manual.pdf

[11] ARIA Reference manual [Online]. Available: http://robots.mobilerobots.com/ArPowerCube/ArPowerCube-Reference.pdf..

[12] Rehbinder, H., Ghosh, B.K, "Multi-rate fusion of visual and inertial data," Multisensor Fusion and Integration for Intelligent Systems, 97-102 (2002)

[13] Rehbinder, H., Ghosh, B.K, "Pose Estimation Using Line-Based Dynamic Vision and Inertial Sensors," IEEE Tran. Automatic Control, VoL. 48, NO.2, 2003

[14] C. R. Rao, H. Toutenburg, A. Fieger, C. Heumann, T. Nittner and S. Scheid, *Linear models: Least Squares and Alternatives.* Spring Series in Statistics, 1999